Preprints of the 21st IFAC World Congress (Virtual)
Berlin, Germany, July 12-17, 2020

Nonlinear Model Predictive Control for the Landing of a Quadrotor on a Marine Surface Vehicle

Giuseppe Gillini, Filippo Arrichiello

University of Cassino and Southern Lazio,
Department of Electrical and Information Engineering,
Via G. Di Biasio 43, 03043 Cassino (FR), Italy
{giuseppe.gillini, f.arrichiello}@unicas.it.

Abstract:
The paper addresses the design of a control strategy for a quadrotor autonomous aerial vehicle to land on a target marine surface vehicle. In particular, a Nonlinear Model Predictive Control law that takes into account the marine vehicle trajectory and the sea state has been designed to let the quadrotor land on the target vehicle when this reaches a wave peak. The sea state has been modeled using monochromatic sinusoidal waves, and the maximum wave height and period are taken into account by the quadrotor control law to compute the position and the timing of the next vertical peak in the target vehicle trajectory. The results of numerical simulations performed in ROS/Gazebo environment are shown to validate the control strategy effectiveness.

Keywords: Predictive Control, Automatic Control, Robotics, Mobile Robots, Optimal Control.

1. INTRODUCTION

In the recent years, Unmanned Aerial Vehicles (UAVs) are playing an important role in many applications, as described in Leutenegger et al. (2016), like inspection and monitoring, Simultaneous Localization and Mapping (SLAM) of unknown environments, precise agriculture and so on. Here, we focus on specific applications involving the marine environment, as the use of UAVs for coastal monitoring or water sampling, e.g. see Casella et al. (2016) or Ribeiro et al. (2016). Among the different classes of UAVs, quadrotors represent one of the most largely used type of UAVs due to their capability of hovering and vertical take off and landing; however, due to their reduced autonomy in term of batteries endurance, when quadrotor UAVs are required to perform an operation far from the sea coast, it might be useful to transport them with a different vehicle (e.g. a marine surface vessel) and take them off only in proximity of the area of interest.

Autonomous take off and landing of a quadrotor on a moving target represents an interesting research topic, since it involves both control and perception issues. Indeed, to allow the quadrotor to land on a moving vehicle, the relative positioning between the UAV and the landing platform needs to be estimated, and a control solution that takes into account the motions of both the systems must be developed. Common approaches for relative positioning estimation are based on visual servoing techniques, as in Lee et al. (2012) and in Falanga et al. (2017) where the target position is obtained relying on state-of-the-art computer vision algorithms. In Polvara et al. (2018) an extended Kalman filter estimates the current target vehicle position with reference to the last known position, also taking into account the relative position measurements gained using fiducial markers placed on the landing platform.

Concerning the landing control strategy, when the landing platform is on a marine vehicle subjected to oscillations due to the sea state, it is appropriate to define when the quadrotor has to perform the landing. Different approaches to face the problem of landing on an oscillating platform are shown in the works Lippiello and Ruggiero (2016) and Nisticò et al. (2017). In Cabecinhas et al. (2016) a robust controller for a quadrotor landing maneuver has been developed where the control law switches according to the type of contact with the ground.

Among the possible landing control strategies, here we want to focus on the use of Nonlinear Model Predictive Control (NMPC) techniques. The main idea of MPC is to utilize a model of the process in order to predict and optimize the future system behavior. Thanks to its versatility, MPC has been used for a large class of applications, as in Plessen and Bemporad (2017) where a MPC strategy for the control of an autonomous and slowly moving agricultural machinery is presented, or as in Jain et al. (2017) where an NMPC approach is employed by an Autonomous Underwater Vehicle (AUV) to track and to estimate a moving target using range measurements. NMPC control law could be also used to solve the moving path following motion control problem, as in Jain et al. (2018) where a robotic vehicle is required to converge to a desired geometric path, expressed with respect to a moving frame of reference, while satisfying the actuation constraints.

In this paper we aim at designing a NMPC strategy for a quadrotor UAV to realize the landing of the quadrotor on a moving marine vehicle when it reaches the Maximum Wave Height (MWH). To the purpose, the sea state is taken into account to estimate the target vehicle motion, and the control law is designed to allow the quadrotor to firstly approach the marine vehicle, by aligning in the horizontal plane and reaching a threshold altitude from the maximum of the sea wave, and, then, to land on the marine vehicle when the latter reaches the MWH. Despite the sea state estimation is out of the scope of this work, it is worth remarking that different approaches to estimate the main sea parameters can be used, as Wang et al. (2010) and Liu et al. (2015). The results of numerical simulations performed in Gazebo environment, using the open-source framework for the dynamic optimization ACADO Houska et al. (2011), is presented to validate the effectiveness of the proposed solution.

This paper is organized as follow: Section 2 describes the system modeling while Section 3 presents the landing control strategy. Numerical simulation results are presented in Section 4, while Section 5 concludes the paper.

2. SYSTEM MODELING

This section discusses the modeling of the quadrotor dynamics, the sea state and the target marine vehicle motion.

2.1 Quadrotor Model

Let's consider an inertial frame $\mathbf{E}_i$ and a body frame $\mathbf{E}_b$ attached to the quadrotor (Fig. 1).

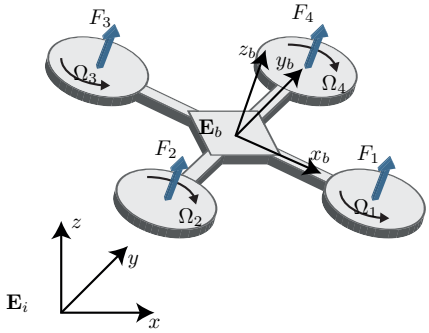

Fig. 1. Inertial and body frame with respect to the quadrotor and its parameters.

The vectors containing the 3D position and the Euler angles roll, pitch and yaw of the quadrotor with respect to the inertial frame are respectively defined as $\mathbf{p}_q = [p_{q,x}\ p_{q,y}\ p_{q,z}]^T$, $\rho_q = [\phi\ \theta\ \psi]^T$. From 3D body kinematics, it follows that the linear and the angular velocities in the two reference frames are linked by the following relations:

$$\mathbf{v}_q = \mathbf{R}\mathbf{v}_b \tag{1}$$

$$\dot{\rho}_q = \mathbf{T}\omega_b \tag{2}$$

where $\mathbf{v}_q = [\dot{x}\ \dot{y}\ \dot{z}]^T \in \mathbb{R}^3$ is the linear velocity and $\dot{\rho}_q = [\dot{\phi}\ \dot{\theta}\ \dot{\psi}]^T \in \mathbb{R}^3$ the rate of change of Euler angles in inertial frame; $\mathbf{v}_b = [u\ v\ w]^T \in \mathbb{R}^3$, $\omega_b = [p\ q\ r]^T \in \mathbb{R}^3$ are linear and angular velocity in body frame; $\mathbf{R}$ is the rotation matrix from the body reference system to the inertial reference and $\mathbf{T}$ is the angular transformation matrix.

The actuator dynamics is given by

$$\begin{cases} f_t = b(\Omega_1^2 + \Omega_2^2 + \Omega_3^2 + \Omega_4^2) \\ \tau_x = bl(\Omega_1^2 - \Omega_3^2) \\ \tau_y = bl(\Omega_2^2 - \Omega_4^2) \\ \tau_z = d(\Omega_1^2 + \Omega_3^2 - \Omega_2^2 - \Omega_4^2) \end{cases} \tag{3}$$

where l is the distance between any rotor and the center of the quadrotor, b is the thrust factor, d is the drag factor and Ω_i is the angular speed of the ith rotor.

Defining as $\mathbf{f}_b = [0\ 0\ f_t]^T$ the vector containing the thrust force in body frame and $\tau_b = [\tau_x\ \tau_y\ \tau_z]^T$ the vector containing the torques in body frame, the dynamical model of a quadrotor is:

$$m\dot{\mathbf{v}}_q = m\mathbf{g} + \mathbf{R}\mathbf{f}_b - \mathbf{K}_{d,f}\mathbf{v}_q \tag{4}$$

$$\tau_b - \mathbf{K}_{d,m}\omega_b = \mathbf{I}\dot{\omega}_b + \omega_b \times \mathbf{I}\omega_b \tag{5}$$

where $\mathbf{g} = [0\ 0\ -g]$ is the gravity vector, $\mathbf{I}$ is the inertia matrix, $\mathbf{K}_{d,f}$ and $\mathbf{K}_{d,m}$ are the matrices containing the coefficients of the drag forces and torques.

2.2 Sea state modeling

A sea wave can be described by the spatio - temporal evolution of the sea surface's height with respect to the sea level. In particular, defining as h the sea surface's height, a monochromatic sinusoidal wave is mathematically represented in the following form:

$$h(x, y, t) = A\ cos(\mathbf{k}^{\mathrm{T}} \cdot \mathbf{r} - \omega_{\mathrm{sea}}(\mathbf{k})t + \varphi) \tag{6}$$

where A is the maximum wave amplitude, $\mathbf{r} = [r_x\ r_y]^T$ is the vector of the horizontal sea coordinates, ω_{sea} and φ respectively are the angular frequency and the phase of the sea wave, and $\mathbf{k} = [k_x\ k_y]^T$ is the wave vector pointing in the propagation direction of the wave. In particular $\mathbf{k}$ is related to the wave length λ by the following equation

$$|\mathbf{k}| = \frac{2\pi}{\lambda}. \tag{7}$$

Moreover, in deep water conditions, a specific relationship between the frequency and the wave vector holds:

$$\omega_{\mathrm{sea}}^2(\mathbf{k}) = g\,|\mathbf{k}| \tag{8}$$

where g is the gravitational acceleration.

The wave period T could be evaluated as:

$$T = \frac{2\pi}{\mathbf{k}^T \cdot \mathbf{v}_{\mathrm{sea}}} \tag{9}$$

where $\mathbf{v}_{\mathrm{sea}}$ is the wave propagation velocity defined as:

$$|\mathbf{v}_{\mathrm{sea}}| = \frac{\omega_{\mathrm{sea}}(\mathbf{k})}{|\mathbf{k}|}. \tag{10}$$

2.3 Marine Vehicle Model

In this work, as a first approximation, the target vehicle has been modeled as 3-DOF kinematic model, treating it as a material point and ignoring its orientation. Thus, defining as $\mathbf{p}_t = [p_{t_x}\ p_{t_y}\ p_{t_z}]^T$ the vehicle position and

$\mathbf{v}_t$ the linear velocity, the following ODE problem will be obtained:

$$\begin{aligned} \dot{p}_{t_x}(t) &= v_{t_x} \\ \dot{p}_{t_y}(t) &= v_{t_y} \\ \dot{p}_{t_z}(t) &= v_{t_z} \end{aligned} \tag{11}$$

In particular, v_{t_x} and v_{t_y} are treated as constant inputs for the vehicle, while p_{t_z} and v_{t_z} evolves according to the wave height shape.

3. LANDING CONTROL ALGORITHM

3.1 Control algorithm

The landing maneuver is decomposed into two different stages. In the first stage, the control law is designed to let the quadrotor approach the marine vehicle by aligning in the horizontal plane and by reaching a threshold altitude from the maximum of the sea wave; in the second stage, the control law, on the base of the sea state and of the marine vehicle's trajectory, let the quadrotor land when the vehicle reaches one of the MWHs.

The control law applied to the quadrotor is an NMPC law with the optimization problem structured as in the following:

$$\begin{aligned} \min_{\mathbf{z}} \quad & \textstyle\sum_{k=0}^{N-1} \Gamma(\mathbf{x}_k, \mathbf{u}_k) + F(\mathbf{x}_N) \\ \text{s.t.} \quad & \mathbf{x}_{k+1} = f(\mathbf{x}_k, \mathbf{u}_k) \\ & \mathbf{u}_k \in \mathcal{U},\ \mathbf{x}_k \in \mathcal{X},\ \mathbf{x}_N \in \mathcal{X}_f \end{aligned} \tag{12}$$

where Γ and F are the stage and the terminal costs designed to address the two different stages and whose specific formulations will be discussed later in this session; $f(\mathbf{x}_k, \mathbf{u}_k)$ is the discretized dynamic model of the quadrotor shown in subsection 2.1; $\mathbf{u}_k$ is the control input vector defined as $\mathbf{u}_k = [f_t\ \tau_x\ \tau_y\ \tau_z]^T$; $\mathbf{x}_k$ is the state vector defined as $\mathbf{x}_k = [\mathbf{p}_q\ \mathbf{v}_q\ \rho_q\ \omega_b]^T$; $\mathbf{z} = [\mathbf{u}_{0|k}\ \mathbf{u}_{1|k}\ \mathbf{u}_{2|k}\ \dots\ \mathbf{u}_{N-1|k}]$ is a control sequence with horizon N; $\mathcal{U}$, $\mathcal{X}$, $\mathcal{X}_f$ respectively are the control inputs, state and terminal cost feasible sets (the set of all possible points of the optimization problem that satisfy the problem's constraints). The notation $\mathbf{u}_{i|k}$ means the ith result of the optimization problem computed at k instant. The optimization problem is solved at each sampling instant, thus computing the optimal control along the horizon N starting from the current configuration, but only the first value of the control sequence is then effectively applied.

With reference to Fig. 2, the MWH is referred as $A_{\max}$, while A_{ref} is a properly designed, fixed reference height from the sea level. The quadrotor is intially commanded to align its horizontal position with the one of the marine vehicle and to hover on it at an altitude A_{ref}. When such configuration is reached, according to a specified threshold, the control law takes into account the sea state and the marine vehicle trajectory to compute when it will reach the next MWH, and it commands the UAV to land on it.

In particular, the second stage of the landing procedure works as in the following. Denoting as $T_{\max}$ the time distance between two peaks of the target vehicle vertical motion, from equation (9) this could be expressed as:

$$T_{\max} = \frac{2\pi}{\mathbf{k}^T \cdot \mathbf{v}_{\text{diff}}} \tag{13}$$

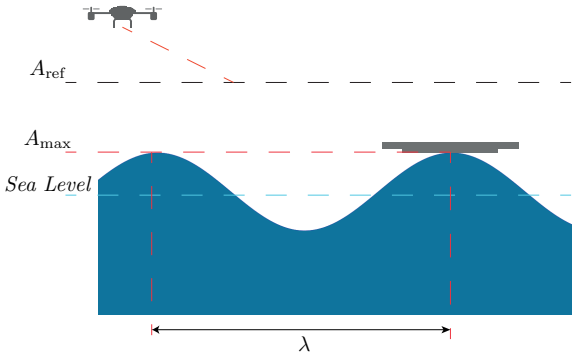

Fig. 2. Sea wave snapshot with its parameters taking into account for the control algorithm: A_{ref} is a fixed reference height from the sea level, $A_{\max}$ is the maximum wave height (MWH).

where $\mathbf{k}$ is the wave vector and $\mathbf{v}_{\text{diff}}$ is the offset between the velocity of the marine vehicle in the horizontal plane and the propagation velocity of the sea wave.

Denoting as $N_{\max}$ the number of time steps between the current time instant and time instant of the next peak in the target vertical trajectory, this is calculated as:

$$N_{\max} = \lfloor \frac{T_{\text{to\_peak}}}{T_s} \rfloor \tag{14}$$

where $\lfloor \cdot \rfloor$ is the floor function, T_s is the sampling time and $T_{\text{to\_peak}}$ is the time distance from the next time instant where the vehicle trajectory reaches its next maximum height. A physical interpretation of these parameters is shown in the Fig. 3.

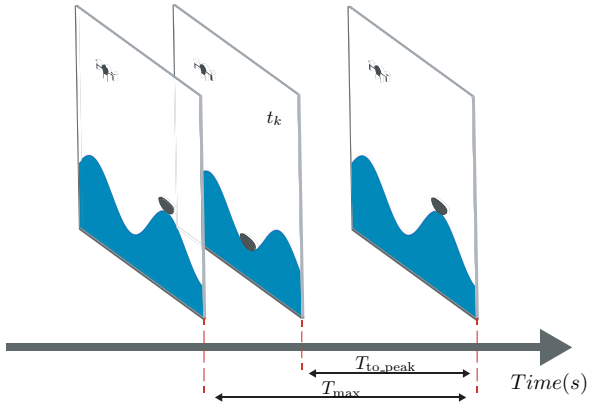

Fig. 3. Different sea wave snapshots. Considering the time instant t_k, $T_{\text{to\_peak}}$ is the time distance from the next time instant where the vehicle trajectory reaches its next maximum height. $T_{\max}$ is the time distance between two peaks of the target vehicle trajectory.

At each instant k, the $N_{\max}$ and $T_{\max}$ values are taken as input for the sequence of instructions that describe the algorithm. The control algorithm will check if the prediction horizon N of the NMPC law is greater or smaller than the number of instants from that value, $N_{\max}$. This difference is described through the parameter γ, and it is evaluated as:

$$\gamma = N - N_{\max}. \tag{15}$$

If γ is greater than 0, it means that the next trajectory peak is in the predicted horizon of the NMPC law, so the

quadrotor will be able to land on the marine vehicle. Else, if γ is lower than 0, then the next peak is outside from the prediction horizon, so the reference for the z coordinate of the quadrotor will be kept at the reference height A_{ref}. A representation of this landing procedure is shown in the Fig. 4.

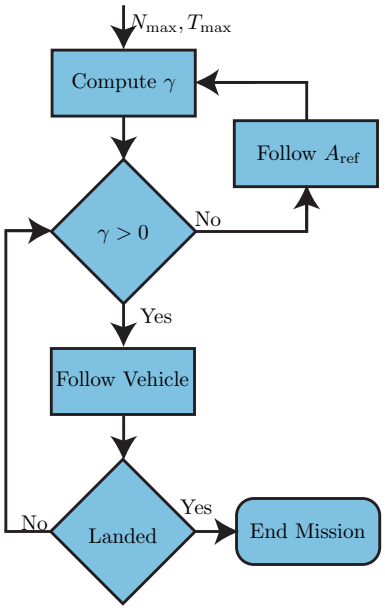

Fig. 4. Second stage of the landing procedure described in the subsection 3.1.

The stage and terminal costs in Eq. (12) can be formulated as in the following:

$$\begin{aligned}\Gamma(\mathbf{x}_k, \Delta\mathbf{u}_k) = &(\mathbf{x}_k - \mathbf{x}_r)^T \mathbf{Q}_{B,\gamma}(\mathbf{x}_k - \mathbf{x}_r) \\ &+ (\mathbf{x}_k - \mathbf{x}_{r_A})^T \mathbf{Q}_{A,\gamma}(\mathbf{x}_k - \mathbf{x}_{r_A}) \\ &+ \Delta\mathbf{u}_k^T \mathbf{Q}_u \Delta\mathbf{u}_k\end{aligned} \tag{16}$$

$$\begin{aligned}F(\mathbf{x}_N) = &(\mathbf{x}_N - \mathbf{x}_r)^T \mathbf{Q}_{N_B,\gamma}(\mathbf{x}_N - \mathbf{x}_r) \\ &+ (\mathbf{x}_N - \mathbf{x}_{r_A})^T \mathbf{Q}_{N_A,\gamma}(\mathbf{x}_N - \mathbf{x}_{r_A})\end{aligned} \tag{17}$$

where $\mathbf{x}_r = [\mathbf{p}_{t,B}\ \mathbf{v}_{t,B}\ \mathbf{0}_3\ \mathbf{0}_3]^T$ is the reference with respect to the target vehicle; $\mathbf{x}_{r_A} = [\mathbf{p}_{t,A}\ \mathbf{v}_{t,A}\ \mathbf{0}_3\ \mathbf{0}_3]^T$ is the reference with respect to the target vehicle's next trajectory peak; $\mathbf{p}_{t,B} = \begin{bmatrix} p_{t_x} + \delta_{p_x} & p_{t_y} + \delta_{p_y} & A_{\text{ref}} \end{bmatrix}$, $\mathbf{v}_{t,B} = \begin{bmatrix} v_{t_x} & v_{t_y} & 0 \end{bmatrix}$, $\mathbf{p}_{t,A} = \begin{bmatrix} p_{t_x} + \delta_{p_x} & p_{t_y} + \delta_{p_y} & p_{t_z} \end{bmatrix}$, $\mathbf{v}_{t,A} = \begin{bmatrix} v_{t_x} & v_{t_y} & v_{t_y} \end{bmatrix}$, $\mathbf{0}_3 = [0\ 0\ 0]$ and $\delta_p = \begin{bmatrix} \delta_{p_x} & \delta_{p_y} \end{bmatrix}^T$ is a virtual point position located in front of the target vehicle to allow the quadrotor to correctly tracking it. $\mathbf{Q}_u$ is the weight matrix for the control input ($\mathbf{Q}_u \succ 0$) and $\Delta\mathbf{u}_k \triangleq \mathbf{u}_k - \mathbf{u}_{k-1}$. $\mathbf{Q}_{B,\gamma}$ and $\mathbf{Q}_{A,\gamma}$ are the weight matrices for the state variables error, defined as:

$$\mathbf{Q}_{B,\gamma} = \xi \mathbf{Q}_B \tag{18}$$

$$\mathbf{Q}_{A,\gamma} = (1 - \xi)\mathbf{Q}_A \tag{19}$$

with:

$$\xi = |\text{sgn}(\gamma)| \frac{1 - \text{sgn}(\gamma)}{2}. \tag{20}$$

In particular, $\mathbf{Q}_B$ and $\mathbf{Q}_A$ are constant weight matrices, and it holds:

$$\mathbf{Q}_{B,\gamma} = \begin{cases} \mathbf{0}, & \text{if } \gamma \geq 0 \\ \mathbf{Q}_B, & \text{if } \gamma < 0 \end{cases}$$

$$\mathbf{Q}_{A,\gamma} = \begin{cases} \mathbf{Q}_A, & \text{if } \gamma \geq 0 \\ \mathbf{0}, & \text{if } \gamma < 0 \end{cases}$$

$\mathbf{Q}_{N_A,\gamma}$ and $\mathbf{Q}_{N_B,\gamma}$ are the weight matrices for the terminal cost designed in the same way of $\mathbf{Q}_{B,\gamma}$ and $\mathbf{Q}_{A,\gamma}$.

3.2 Stability

Since the switching weight matrices of the cost functions are mutually exclusive, the NMPC control law could be treated as a two stages NMPC problem. In particular, in the first stage, the quadrotor has to align its horizontal coordinates with the marine vehicle, reaching an altitude equal to A_{ref}; while in the second stage, the quadrotor has to perform the effective landing, reaching an altitude equal to A_{max}. It is worth noticing that A_{ref} should be design to let the quadrotor be able to land (changing its altitude from A_{ref} to A_{max}) in a time frame equal to the prediction horizon, without violating feasibility constraints, in such a way to let the control law switch just once. We address the stability of the two stages by shifting the origin of the problem once in $\mathbf{x}_r$ and once in $\mathbf{x}_{r_A}$, and by applying the standard MPC scheme on the translated system, as in Simon et al. (2012), considering the active part of stage and terminal cost functions. The stability result of each stage could be addressed by the standard Lyapunov based stability proof for NMPC.

4. SIMULATION RESULTS

This section presents the results of a numerical simulation performed using Gazebo environment through the Robot Operating System (ROS), with the ACADO Toolkit, using the control strategy presented in section 3.

The sea wave has been simulated through the asv_wave_sim plugin [1] . The MWH and the wave vector have been treated like known parameters chosen as $\mathbf{k}^T = [1\ 1]$ and MWH = 0.50 m. A_{ref} has been fixed at 1.50 m in such a way that in the MWH condition the height distance between the marine vehicle and the quadrotor is adequate to attend the landing maneuver. The marine vehicle is supposed to move in the horizontal plane with velocities $v_{t_x} = 0.5$ m/s and $v_{t_y} = 0$ m/s. The quadrotor has been modeled with the dynamical parameters shown in Table 1.

Table 1. Dynamical Parameters Quadrotor

Parameter	Value	um
I_{xx}	0.01	$\text{kg} \cdot \text{m}^2$
I_{yy}	0.01	$\text{kg} \cdot \text{m}^2$
I_{zz}	0.02	$\text{kg} \cdot \text{m}^2$
b	8.06×10^{-5}	kg/m
d	1.00×10^{-6}	kg/m
l	0.21	m
m	1	kg

The sampling time of the simulation has been set to $T_s = 0.10$ s and the prediction horizon N of the NMPC control law has been set to 20 steps. The stage cost and terminal cost gains are chosen equal to $\mathbf{Q}_B = \mathbf{Q}_A = \mathbf{Q}_N = 10.00 \begin{bmatrix} 10\,\mathcal{I}_3 & \mathbf{O}_{3\times9} \\ \mathcal{I}_9 & \mathbf{O}_{9\times3} \end{bmatrix}$, $\mathbf{Q}_u = 1\ \mathcal{I}_4$, where $\mathcal{I}_n$ is the identity

[1] https://github.com/srmainwaring/asv_wave_sim

matrix of size $n \times n$ and $\mathbf{O}_{n\times m}$ is the zero matrix of size $n \times m$.

The initial position of the quadrotor has been set away from the starting point of the target vehicle and with an altitude greater than A_{ref}. In this way, the quadrotor has to follow each step of the control procedure in subsection 3.1. In fact, first the quadrotor reaches the A_{ref} value while its x, y position follow the x, y position of the target vehicle, then it can try to land on marine vehicle when it reaches the next wave peak.

Fig. 5 shows the vertical coordinates of the quadrotor and marine vehicle, highlighting the reference height values, the reference switch and the landing time instant. Note that the height offset between the marine vehicle and the quadrotor, visible after the landing, is due to the height difference between the landing platform of the marine vehicle and the position of the quadrotor control point, placed in its centroid.

Fig. 6 shows the value of the variable $\text{sgn}(\gamma)$ that changes according to the time distance from next MWH. Such parameter plays a key role since it allows the switching of the matrix gains and the control law references. When γ has switched its value, the quadrotor should be ready to land unless its horizontal coordinates are not aligned with those of the target vehicle.

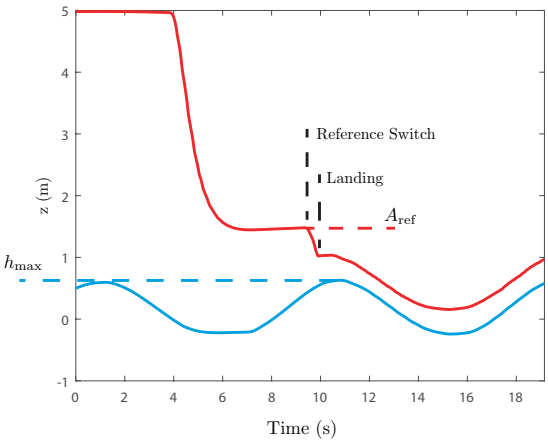

Fig. 5. Vertical coordinates of Quadrotor (red line) and moving vehicle (blu line) with respect to time. The plot also shows A_{ref} and $h_{\max}$, namely the maximum marine vehicle's height read from the on-board sensors.

Fig. 7 and Fig. 8 show the computed control inputs as thrust and torques, while Fig. 9 shows a sequence of snapshots of the mission execution simulated in Gazebo.

A video showing the simulation results is available at: `https://youtu.be/eKKDV3-K_M4`.

5. CONCLUSION

This work presented a way to use a nonlinear model predictive control law to allow a quadrotor to land on a marine moving vehicle considering the sea state. In particular, taking into account the sea wave vector and the MWH, the quadrotor is able to land on the target vehicle when

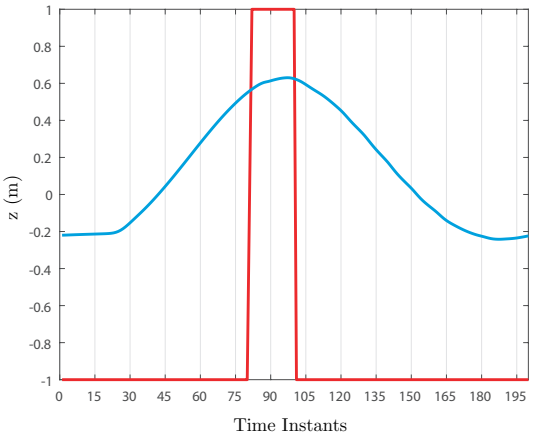

Fig. 6. Vertical coordinate of the marine vehicle trajectory in meters (blue line) and the $\text{sgn}(\gamma)$ function (red line).

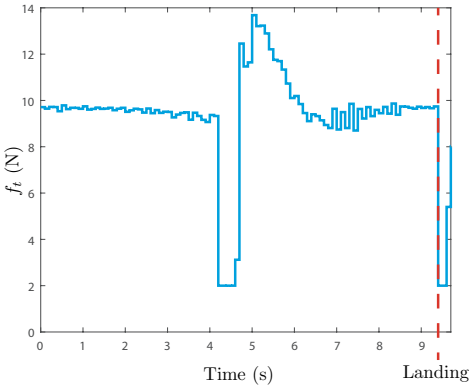

Fig. 7. Total thrust f_t computed by the NMPC control law.

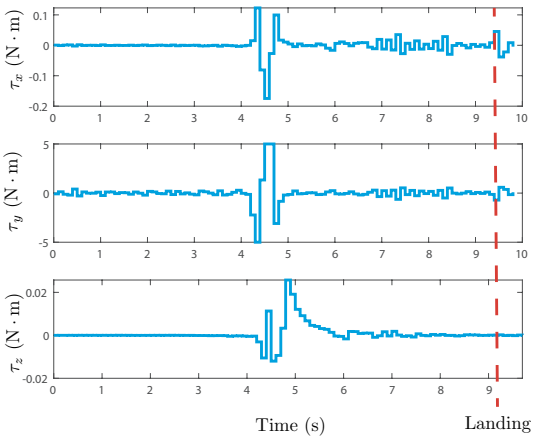

Fig. 8. Torques τ_x, τ_y, τ_z computed by the NMPC control law.

it reaches the maximum altitude. Future works will focus on the integration of online sea state estimation techniques with the information gathered from on board sensors of the target vehicle, and on the inclusion of the attitude in the marine vehicle dynamic modeling. Moreover, experimental validation is forecast in the framework of the interna-

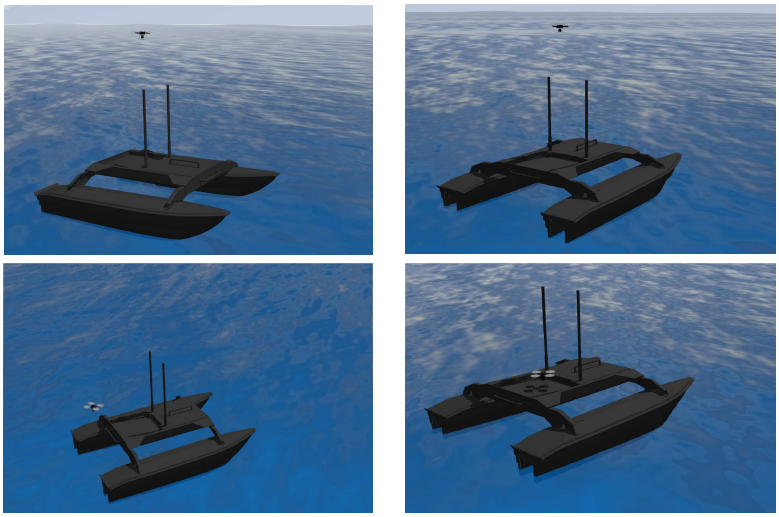

Fig. 9. Sequence of snapshots of the mission execution simulated in ROS Gazebo.

tional project TARMEM granted by the Qatar National Research Fund.

ACKNOWLEDGMENT

This work was made possible by NPRP grant #10-0213-170458 (TARMEM project) from the Qatar National Research Fund (a member of Qatar Foundation). The findings herein reflect the work, and are solely the responsibility of the authors.

REFERENCES

Cabecinhas, D., Naldi, R., Silvestre, C., Cunha, R., and Marconi, L. (2016). Robust landing and sliding maneuver hybrid controller for a quadrotor vehicle. *IEEE Transactions on Control Systems Technology*, 24(2), 400–412.

Casella, E., Rovere, A., Pedroncini, A., Stark, C.P., Casella, M., Ferrari, M., and Firpo, M. (2016). Drones as tools for monitoring beach topography changes in the ligurian sea (nw mediterranean). *Geo-Marine Letters*, 36(2), 151–163.

Falanga, D., Zanchettin, A., Simovic, A., Delmerico, J., and Scaramuzza, D. (2017). Vision-based autonomous quadrotor landing on a moving platform. In *Proceedings of the IEEE International Symposium on Safety, Security and Rescue Robotics, Shanghai, China*, 11–13.

Houska, B., Ferreau, H.J., and Diehl, M. (2011). Acado toolkitan open-source framework for automatic control and dynamic optimization. *Optimal Control Applications and Methods*, 32(3), 298–312.

Jain, R.P., Alessandretti, A., Aguiar, A.P., and de Sousa, J.B. (2017). A nonlinear model predictive control for an auv to track and estimate a moving target using range measurements. In *Iberian Robotics conference*, 161–170. Springer.

Jain, R.P.K., Aguiar, A.P., Alessandretti, A., and Borges de Sousa, J. (2018). Moving path following control of constrained underactuated vehicles: A nonlinear model predictive control approach. In *2018 AIAA Information Systems-AIAA Infotech@ Aerospace*, 0509.

Lee, D., Ryan, T., and Kim, H.J. (2012). Autonomous landing of a vtol uav on a moving platform using image-based visual servoing. In *IEEE International Conference on Robotics and Automation (ICRA), 2012*, 971–976. IEEE.

Leutenegger, S., Hürzeler, C., Stowers, A.K., Alexis, K., Achtelik, M.W., Lentink, D., Oh, P.Y., and Siegwart, R. (2016). Flying robots. In *Springer Handbook of Robotics*, 623–670. Springer.

Lippiello, V. and Ruggiero, F. (2016). Orbital stabilization of a VToL UAV for landing on oscillating platforms. In *IEEE International Symposium on Safety, Security, and Rescue Robotics (SSRR), 2016*, 131–138. IEEE.

Liu, X., Huang, W., and Gill, E.W. (2015). Shadowing-analysis-based wave height measurement from ship-borne x-band nautical radar images. In *OCEANS 2015-Genova*, 1–4. IEEE.

Nisticò, A., Baglietto, M., Simetti, E., Casalino, G., and Sperindè, A. (2017). Marea project: Uav landing procedure on a moving and floating platform. In *OCEANS–Anchorage, 2017*, 1–10. IEEE.

Plessen, M.M.G. and Bemporad, A. (2017). Reference trajectory planning under constraints and path tracking using linear time-varying model predictive control for agricultural machines. *Biosystems Engineering*, 153, 28–41.

Polvara, R., Sharma, S., Wan, J., Manning, A., and Sutton, R. (2018). Vision-based autonomous landing of a quadrotor on the perturbed deck of an unmanned surface vehicle. *Drones*, 2(2), 15.

Ribeiro, M., Ferreira, A.S., Gonçalves, P., Galante, J., and de Sousa, J.B. (2016). Quadcopter platforms for water sampling and sensor deployment. In *OCEANS 2016 MTS/IEEE Monterey*, 1–5. IEEE.

Simon, D., Löfberg, J., and Glad, T. (2012). Reference tracking mpc using terminal set scaling. In *IEEE 51st Annual Conference on Decision and Control (CDC), 2012*, 4543–4548. IEEE.

Wang, F., Wang, J., and Wang, S. (2010). Estimation of significant wave height from x-band marine radar images. In *3rd International Congress on Image and Signal Processing (CISP), 2010*, volume 5, 2172–2174. IEEE.